


Perspective

Photocatalytic and Thermo-Photocatalytic Processes: Advantages of Modelling Light Irradiation and Temperature Profiles

Mario J. Muñoz-Batista 

Department of Chemical Engineering, University of Granada, 18074 Granada, Spain; mariomunoz@ugr.es

Abstract: This contribution presents a personal perspective on the development of thermo-photocatalytic schemes. It discusses several concepts focused on the common presentation of catalytic and thermo-photocatalytic data, with special emphasis on the determination of TOF (Turnover Frequency) and Quantum Efficiency parameters. The importance of including temperature profiles and photon absorption rates in the analysis for intrinsic kinetic studies, comparison of catalytic results, and the potential scaling of reactors is highlighted. Additionally, topics related to the efficiency of the use of radiation and heat transfer are discussed. Photon absorption profiles are presented for a TiO₂ catalytic surface of 20 × 20 cm (both fluorescent and LED configuration), as well as the temperature profile obtained using a thermal resistance with a diameter of 5 cm in a flat reactor. Using this example, the importance of designing thermo-photocatalytic systems to ensure an acceptable level of homogeneity in light irradiation and temperature is discussed. The discussion provides data that positions thermo-photocatalytic processes in the early stages of research. It is still necessary to advance the understanding of phenomena occurring under mixed temperature and light conditions. Additionally, new materials that meet the required characteristics for each application need to be developed, along with the design of new thermo-photocatalytic reactors.

Keywords: thermo-photocatalysis; modeling of irradiation matter; TOF; quantum efficiency; local superficial rate of photon absorption



Academic Editor: Bo Weng

Received: 22 November 2024

Revised: 16 December 2024

Accepted: 23 December 2024

Published: 24 December 2024

Citation: Muñoz-Batista, M.J. Photocatalytic and Thermo-Photocatalytic Processes: Advantages of Modelling Light Irradiation and Temperature Profiles. *Catalysts* **2025**, *15*, 7. <https://doi.org/10.3390/catal15010007>

Copyright: © 2024 by the author. Licensee MDPI, Basel, Switzerland. This article is an open access article distributed under the terms and conditions of the Creative Commons Attribution (CC BY) license (<https://creativecommons.org/licenses/by/4.0/>).

1. Introduction

Catalysis plays a crucial role in modern chemistry and industry, significantly enhancing the efficiency of chemical reactions [1–3]. The optimization of selectivity/yields and a wide range of operating condition catalysts enable reactions to proceed at faster rates and under advantageous operating conditions, which is essential for the competitive production of a wide range of chemicals, pharmaceuticals, and fuels [4–11]. The development of effective catalysts is fundamental to advancing sustainable and green chemistry, reducing energy consumption, and minimizing environmental impact [2,12,13]. Photocatalysis, a subset of catalysis, offers several advantages, including the use of mild conditions, as well as the possibility of utilizing efficient irradiation sources or solar radiation. Advances in the design of artificial light sources such as high-efficiency LEDs (Light Emitting Diodes) that can selectively emit light at a specific wavelength open new opportunities for photocatalysis [14–17]. However, the disadvantages and limitations of photocatalysis have been highlighted in numerous studies over the years. The efficiency of photocatalytic reactions is often limited by the low absorption of visible light by many photocatalysts, the rapid recombination of photogenerated electron-hole pairs, and the potential deactivation of catalysts over time [18–24].

Recent advancements in the field have focused on the synergistic effects of combining light and thermal energy to enhance catalytic performance [24–30]. Although the definitions for processes that simultaneously use light and temperature are somewhat ambiguous, and without aiming to be categorical, some approaches used to optimize or investigate multi-energy light–temperature schemes are described below. The approaches address several schemes, including photo-thermal catalysis and plasmonic catalysis, thermo-photocatalysis, and other hybrid schemes (e.g., light-assisted catalysis) [25,26,28,30]. As schematically represented in Figure 1, thermo-photocatalysis involves the simultaneous application of light and heat to a photocatalyst. This scheme aims to utilize thermal energy to potentially enhance the mobility of charge carriers generated by light absorption, thereby improving the overall efficiency of the catalytic process. The heat may also assist in overcoming activation barriers that are not easily surmounted by photonic energy alone. Photothermal catalysis primarily relies on the photothermal effect, where light is absorbed and converted into heat by the catalyst. This localized heating can significantly increase the reaction rates by providing the necessary thermal energy to drive endothermic reactions or to desorb reaction products from the catalyst surface, thus preventing deactivation [26]. Other hybrid schemes include light-assisted thermal catalysis, where light is used to activate the catalyst surface or generate reactive species, while the bulk of the reaction is driven by thermal energy. This approach can be particularly effective in reactions where light alone is insufficient to achieve the desired conversion rates or selectivity. The contribution of the combined use of light and temperature is complex, and as mentioned, it affects both the catalytic sample and all the charge mobility and thermodynamic processes of the reaction.

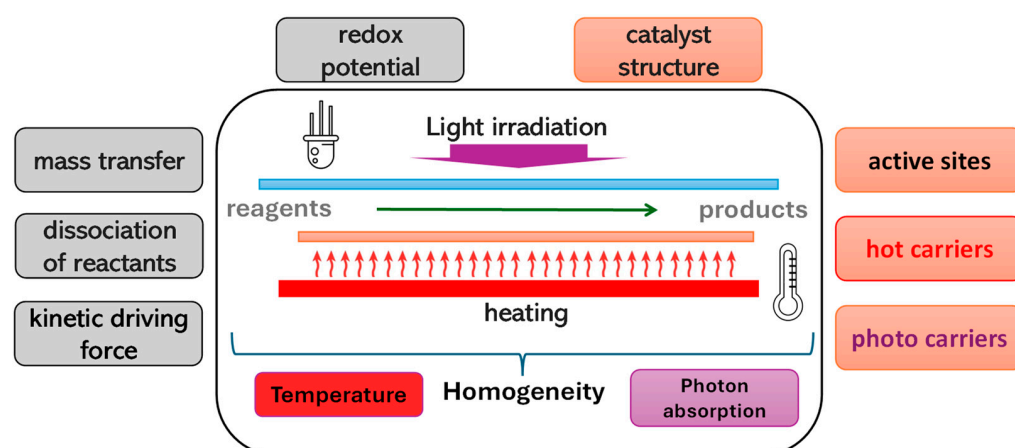


Figure 1. Chemical, structural, and thermodynamic aspects affecting the process mechanism under the combined use of light and temperature. The red text refers to thermocatalytic, while the violet text refers to photocatalytic contributions.

Figure 1 depicts a thermo-photocatalytic reaction scheme in which an external radiation source, specifically a resistance-type heating source, is used. The scheme also introduces an idea addressed throughout this perspective article related to the necessary homogeneity in terms of absorbed radiation and heating of the catalytic surface.

By optimizing the interplay between light and heat, researchers aim to overcome the limitations of traditional photocatalysis, such as low quantum efficiency and catalyst stability, paving the way for more efficient and robust catalytic systems [31–36]. Each of these approaches offers unique advantages and challenges, and ongoing research is focused on understanding the fundamental mechanisms and developing materials that can effectively harness both light and thermal energy.

This article presents a personal perspective on the correct way to evaluate the catalytic properties of processes under light and temperature conditions. It focuses mainly on

heating using thermal resistances and artificial light (e.g., fluorescent lamps or LEDs). It includes the determination of temperature and light absorption profiles on a catalytic film, which can serve as starting points for studying gas-phase processes with supported catalysts, such as hydrogen production schemes, methanation, and degradation of gaseous effluents, among others.

2. How to Normalize the Number of Moles Consumed or Produced: Catalysis vs. Photocatalysis

The Turnover Frequency (TOF) and Quantum Efficiency (η_q) are both critical metrics used to evaluate the efficiency of catalytic (in traditional schemes under high temperature conditions) and photocatalytic processes, respectively [37–40], which permits unrestricted use, distribution, and reproduction in any medium, provided the original work is properly cited. Despite their application in different contexts, they share a fundamental similarity in that both metrics provide a measure of the rate at which a catalyst facilitates a chemical reaction. TOF, defined as the number of moles of product formed per mole of active site per unit of time, offers insight into the intrinsic activity of a catalyst under specific conditions (Equation (1)). In this equation, $\frac{dN_i}{dt}$ is the differential concentration change of i with time, N_{Av} is Avogadro's number and S is the number of active sites. It is crucial to emphasize that the TOF is valid only under specific reaction conditions and reactant concentrations. Therefore, the TOF should be reported alongside the method for measuring surface sites, species concentrations, and the testing conditions.

$$\text{TOF} = \frac{N_{Av}}{S} \frac{dN_i}{dt} \quad (1)$$

Quantum efficiency, defined as the number of desired events (such as product formation) per photon absorbed (*LSRPA*: Local Superficial Rate of Photon absorption, *LVRPA*: Local Volumetric Rate of Photon absorption) provides a measure of the efficiency of a photocatalyst in converting absorbed light into chemical energy (Equation (2)). In this equation, r is the reaction rate expressed as a function of the catalytic area A (e.g., in supported samples) or as a function of the volume V if a catalyst occupies a defined volume (e.g., catalytic suspension or fluid bed). Details related to the simplifications made in the model for determining photon rate should also be described.

$$\eta_q = \frac{\langle r \rangle_{A, V}}{\text{LSRPA or LVRPA}} \quad (2)$$

Both metrics are essential for understanding the performance of catalytic systems, as they account for the efficiency of the catalyst in promoting reactions. Additionally, both TOF and quantum efficiency are influenced by factors such as reaction conditions, catalyst properties, and the nature of the reactants, making them valuable for comparative studies and optimization of catalytic processes. These definitions have significant limitations, and the literature contains numerous confusing reports using both observables [37,38,41,42]. A concise prior analysis highlights the potential for inconsistent calculation methods and the lack of clarity in distinguishing between TOF and Turnover Number (TON), which can lead to misinterpretations of catalytic efficiency and durability [37]. The authors address these issues by proposing uniform definitions and calculation methods, emphasizing the importance of context-specific reporting, and advocating for transparency in experimental conditions. These recommendations aim to facilitate more accurate comparisons of catalysts, optimize their selection for specific applications, and advance understandings of catalytic mechanisms, thereby contributing to more rigorous and reproducible research in the field of catalysis. This approach should also be extrapolated to the study of photocatalytic processes,

where the radiation source introduces numerous new variables. For instance, the type of radiation (fluorescent lights, LEDs, sunlight, etc.) can significantly affect photocatalytic activity [18,43–47]. Each radiation source has different spectral properties, intensities, and energy distributions, which can influence the efficiency and selectivity of the photocatalytic reactions. Additionally, the configuration and geometry of the reactors play a crucial role [48–51]. Factors such as the reactor’s shape, the positioning of the light source, and the distance between the catalyst and the light source can impact the uniformity of light distribution and the overall kinetics reaction. For example, a well-designed reactor can ensure optimal light penetration and minimize shadowing effects, thereby enhancing the photocatalytic performance. Other variables to consider include the wavelength of the light, the intensity and duration of irradiation, and the presence of any light-absorbing or scattering materials within the reactor. These factors can introduce complexities in the experimental setup and data interpretation, making it essential to standardize and clearly report these conditions to enable reproducible and comparable results.

However, despite all these limitations, TOF and quantum efficiency remain highly valuable tools for evaluating the catalytic properties of new processes of interest. Table 1 analyzes the similarities and differences between TOF and quantum efficiency. This table allows readers to quickly identify the advantages and applications of each observable, aiding in the selection and optimization of catalysts for various applications.

Table 1. Comparison of the TOF and quantum efficiency parameter.

Parameter	Turnover Frequency	Quantum Efficiency
	Main Common Points	
Efficiency metrics	Both TOF and quantum efficiency are metrics used to evaluate the efficiency of catalytic processes. They provide <i>quantitative measures</i> of how effectively a catalyst or photocatalyst facilitates a chemical reaction.	
Rate of reaction	TOF and quantum efficiency both relate to the <i>rate at which reactions occur</i> . TOF measures the number of product molecules formed per active site per unit of time, while quantum efficiency measures the number of desired events (such as product formation) per photon absorbed.	
Influence of conditions	Both metrics are <i>influenced by reaction conditions</i> such as temperature (in thermo-photo schemes), pressure, concentration of reactants, and the properties of the catalyst or photocatalyst.	
	Main Differences	
Context of application	TOF is primarily used in thermal and thermo-catalytic processes, where the reaction is driven by heat.	Quantum efficiency is specific to photocatalytic processes, where the light absorbed by the sample initiates the reaction.
Measurement basis	TOF is based on the number of product molecules formed per active site per unit of time, providing a direct measure of catalytic activity.	Quantum efficiency is based on the number of desired events per photon absorbed, focusing on the efficiency of light utilization in driving the reaction.
Units of measurement	TOF is typically expressed in units of s^{-1} , reflecting the frequency of turnover events.	Quantum efficiency is expressed as a percentage, indicating the proportion of absorbed photons that result in the desired chemical transformation (e.g., with a catalyst as a thin-like film; $[\text{mol m}^{-2} \text{s}^{-1}]/[\text{Einstein m}^{-2} \text{s}^{-1}]$).

3. How, Then, Can We Be Strict if the Process Uses Both Energy Sources?

Unfortunately, there is not a clear answer to this question. Even after a careful analysis of related literature, it is not possible to identify a clear trend or consensus on the most stringent way to analyze thermo-photocatalytic processes. The analysis in a thermo-photocatalytic system inherits the main issues of both definitions. The definition of TOF has a problem when considering temperature dependence. A different TOF value for varying thermal conditions limits the potential of this observable to compare catalytic results from different studies. This dependence on the operating conditions is evident in profiles such as those shown in [52]. The TOF profile presented by the authors shows the variation in the calculated TOR for methanol (a), carbon monoxide (b), and methane (c) as a function of temperature and pressure. In strictly photocatalytic processes, this analysis does not make sense, as it is understood that the process takes place under constant and mild temperature and pressure conditions. The analysis becomes more complex in systems where light and temperature are used together. In a multi-energetic process involving both temperature and light, the parameter that is used to evaluate the catalytic properties must account for the combined effects of thermal and photonic energy inputs. This complexity can lead to inconsistencies and challenges in accurately measuring and comparing efficiencies across different experimental setups. Another relevant issue that needs to be addressed is the dependence of optical properties on operating conditions. Previously reported data have presented the absorption spectra for various semiconductors (TiO_2 , ZrO_2 , Nb_2O_5 , Ta_2O_5 , CeO_2 , WO_3 , and ZnO) under different temperature conditions in air [53]. As described by the authors, the absorption edges of each semiconductor shifted toward longer wavelengths at higher temperatures. The relationship between the bandgap and temperature for these semiconductors was also evaluated in this contribution, showing a linear decrease in the bandgap as a function of temperature in all cases. Although the phenomenon is complex, structural studies suggest that the M–O (metal–oxygen) distance exhibits a strong correlation with bandgap narrowing. In contrast, other parameters related to the electronic structure, such as electronegativity, coordination number of metal ions, and valence number of metals, did not significantly affect bandgap narrowing [53]. Even the commonly used methods to estimate, e.g., charge recombination under light excitation, such as photoluminescence analysis or photo-electrochemical measurements, must account for the influence of temperature. This presents an additional challenge regarding the necessary equipment, as many available facilities are not designed to increase the temperature during optical analysis. Figure 2 presents a representative example where modifications affecting charge mobility and optical properties of a Fe-sMoS₂ (3 wt %) sample lead to the development of an efficient thermo-photocatalytic scheme to produce ammonia. Panel (A) shows the amount of exciton (e^-) transfer into N, H, and O as a function of temperature, where a negative value indicates transfer to holes. Panel (B) presents the catalytic performances under different light wavelengths. Panel (C) displays the time-resolved normalized photoluminescence intensity as a function of temperature. Panel (D) features an energy plot of N₂ and water adsorption on Fe-sMoS₂ from DFT calculations, referenced to the energies of Fe-sMoS₂ and free N₂ and water molecules. Finally, panel (E) displays correlation activity with heat and light at pH 7, showing that light directly influences ammonia synthesis through photoexcitation, while heat indirectly affects activity by enhancing the rate and prolonging exciton lifetime [35].

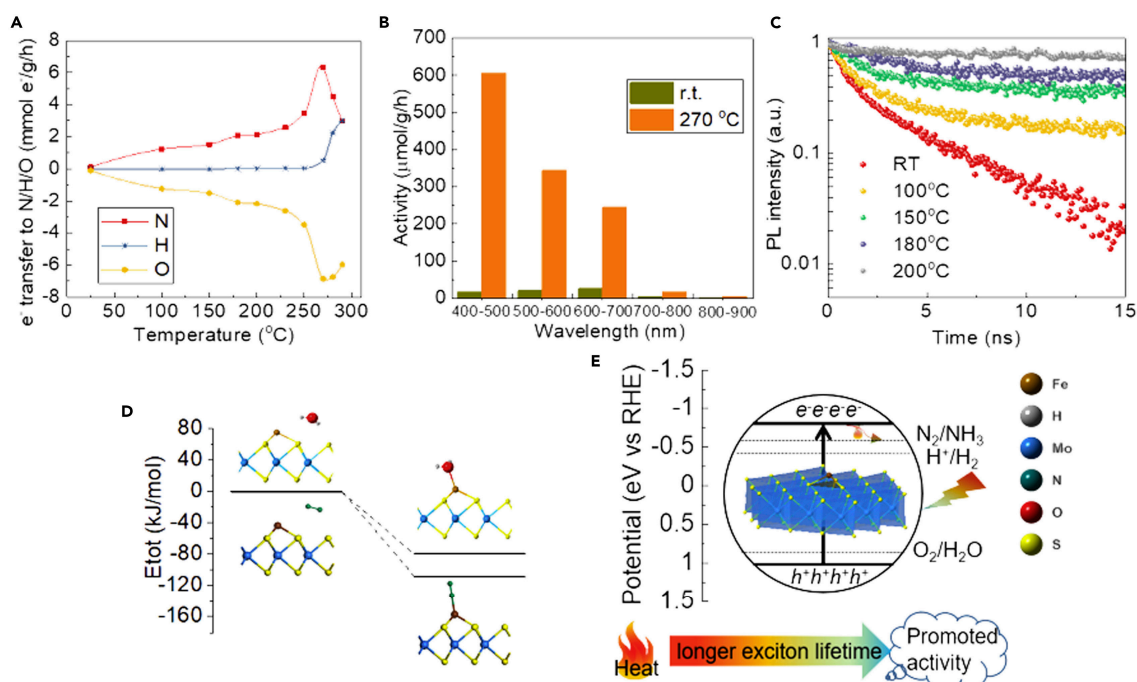


Figure 2. Analysis of several properties under heat and light over Fe-sMoS₂ for ammonia production. (A) Amount of exciton (e⁻) transfer into N, H, and O, (B) catalytic data under combined light and temperature, (C) time-resolved normalized photoluminescence intensity as a function of temperature, (D) energy plot of N₂ and water adsorption on Fe-sMoS₂ from DFT calculations, and (E) correlation of activity with heat and light. Reproduced from [35].

Therefore, while TOF and quantum efficiency are valuable metrics, their application in thermo-photocatalytic systems requires careful consideration of these dependencies to ensure meaningful and comparable results. A possible first approach to address this issue could be to obtain a TOF at a specified temperature by applying the energetic span approximation including a light-related parameter. The energetic span approximation method involves calculating the TOF based on the energy barriers of the elementary steps in the catalytic cycle, providing a way to estimate the TOF by considering the highest energy barrier (rate-determining step) and the overall energy landscape of the reaction pathway (Equation (3)) [54–56].

$$\text{TOF} = \frac{k_B T}{h} \exp\left(-\frac{\delta E}{RT}\right) \quad (3)$$

where k_B is the Boltzmann constant, T is the temperature, h is Planck's constant, δE is the energetic span, defined as the energy difference between the turnover-determining transition state (TDTS) and the turnover-determining intermediate (TDI), and R is the gas constant. In the presence of light, the term “driving force” should indeed include factors related to light absorption. When discussing the driving force in photocatalytic processes, it is indeed more precise to consider the rate of photon absorption. This can be quantified using terms such as the LSRPA or LVRPA as aforementioned. The evaluation of photon absorption profiles has been conducted using various approaches, including phenomenological methods and deterministic or numerical statistical procedures like the Monte Carlo method [57–68]. Although the approaches are varied, one of the strictest involves developing the emission model of the irradiation source and solving the Radiative Transfer Equation (RTE), considering the optical properties of the catalyst, whether in the form of a thin film or a suspension/fluidized bed [69]. With the aim of visualizing the influence of the reactor configuration, Figure 3 shows the calculation of LSRPA profiles

of a TiO_2 sample illuminated with UV radiation generated by fluorescent lamps. This TiO_2 sample, with a measured band gap of 3.0 eV, is deposited as a film on the surface of a quartz plate. The figure shows the photon absorption profile expressed in Einstein $\text{cm}^{-2} \text{s}^{-1}$, obtained using one or several fluorescent lamps with a diameter of 0.8 cm and a length of 20 cm. For the determination of the profiles, it was considered that the lamps are symmetrically positioned from the center of the plate. The model has been solved for a reaction system illuminated by 1, 2, 4 (as shown in the schematic of Figure 3E) and 8 fluorescent lamps. The radiation model and the simplifications used in the model can be seen in detail as described in previous contributions [43].

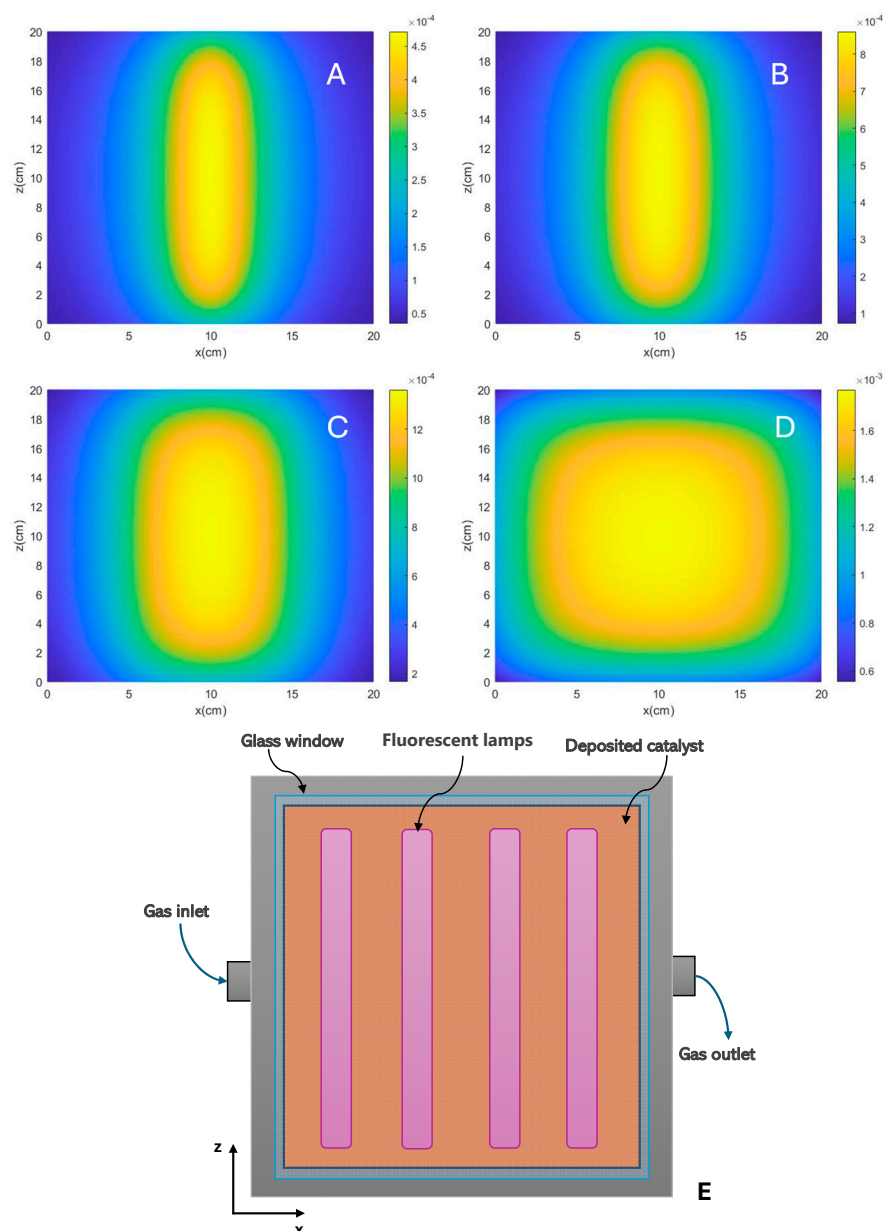


Figure 3. LSRPA calculated for a TiO_2 sample under irradiation of (A) one lamp, (B) two lamps, (C) four lamps and (D) eight lamps. (E) Schematic representation of flat reactor setup system illuminated by four fluorescent lamps.

It is evident that the combined use of light and temperature in catalytic studies introduces specific challenges related to the integration of illumination systems. Light sources must be compatible with high-temperature environments, or must be well-protected, requiring materials that can withstand both thermal and photonic stresses (in any case limited).

The design must also ensure precise alignment between the light source and the sample, particularly when using external systems such as lamps, filters, or fiber optics. Possibly one of the most typical reaction setups, which also enables in situ monitoring of catalytic properties, is the use of high-temperature reaction cells, such as those designed for FTIR spectrophotometers. Figure 4A shows the configuration of a flow reactor in which light and temperature can be used [70]. These types of cells offer a versatile approach to studying catalytic and photocatalytic processes under controlled light and temperature conditions. They support temperatures up to 910 °C and pressures up to 34.4 bar, incorporating features such as gas flow ports for evacuating, pressurizing, or flowing gas through the sample, temperature-controlled stages with integral sample cups, and quartz or ZnSe windows for spectroscopic compatibility [68,70–73]. While this type of system offers great advantages for the study of thermo-photocatalytic processes, it must be considered that the sample is typically arranged as a packed bed, where only a small fraction is directly illuminated under light irradiation conditions. This requires considering an effective light path, which accounts for light attenuation and penetration through the sample [67]. By averaging the photon flux and absorption observables and incorporating the real illumination geometry, an effective light intensity and path profile of the absorbed light can be estimated (Figure 4B). This methodology ensures a more accurate correlation between the optical properties and the observed catalytic performance as it allows the quantification of the amount of light absorbed by the material, identifying areas where, for example, there is no influence of light radiation, and the entire catalytic response is associated with the temperature increase caused by the heating system.

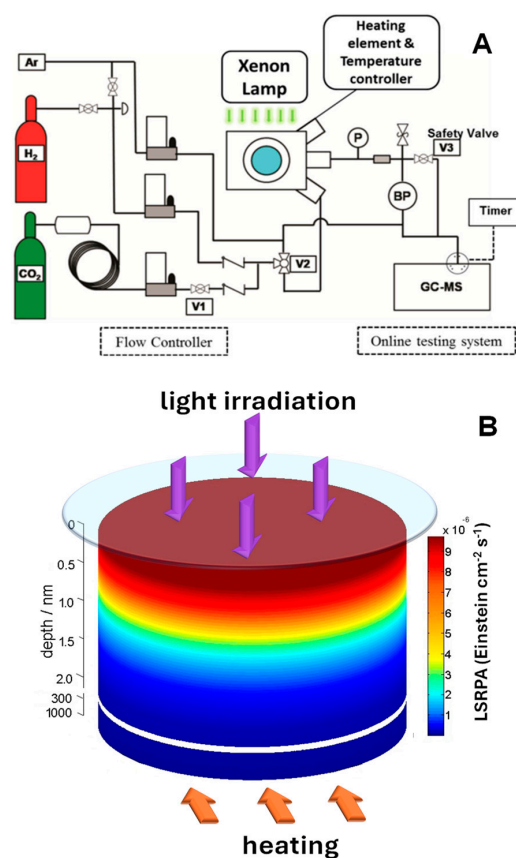


Figure 4. (A) Setup configuration during methanol synthesis over copper/zinc oxide/alumina. Adapted from [70]. (B) Light intensity decay (Einstein cm⁻² s⁻¹) as a function of the depth from the surface of a CuNi/TiO₂ sample. Adapted from [67].

Another widely discussed aspect in the literature concerns scaling factors. Several contributions adopt the thesis that the most convenient procedure involves intrinsic kinetic studies (strictly considering the light–matter interaction in the kinetic equation). Although it is not the only valid approach, validation of scaled data seems to indicate its effectiveness. In this way, the kinetic constants obtained are independent of radiation, thus enabling the scaling of the reaction [74–76]. So, the intrinsic kinetic study approach is crucial for accurately determining reaction rates and mechanisms under controlled conditions. A previous study analyzing advanced spectro-kinetic approaches also describes in detail most of the possible simplifications to obtain these types of intrinsic kinetic equations [69]. By isolating the intrinsic kinetics from external variables such as light intensity, researchers can derive kinetic constants that are truly representative of the reaction’s fundamental behavior. This independence from radiation ensures that the kinetic parameters remain consistent across different scales, facilitating the reliable scaling up of the reaction process. Additionally, in the event that the catalytic material is immobilized, it is advisable for the catalyst to receive radiation uniformly. If the radiation received is uniform across the entire surface, the LSRPA will also be uniform (if the catalytic film is well designed), and a constant average value can be used.

As representative examples, two kinetic equations for 2-propanol degradation are described by Equations (4) (adapted to 2-propanol: C_3H_8O) and (5) [36,69]. Both expressions include the photon rate (LSRPA = $e^{a,s}$). The second equation is used in a contribution where the kinetic analysis is expanded to thermo-photocatalytic systems [36]. As described by Equation (5), under thermo-photo conditions, the kinetic equation must consider both energy sources in the reaction mechanism, providing complex solutions that must be adequately simplified according to the characteristics of the reaction.

$$r_{C_3H_8O} = - \frac{\alpha_1 C_{C_3H_8O} C_{H_2O} \sqrt{e^{a,s}}}{(1 + K_{H_2O} C_{H_2O}) (1 + K_{H_2O} C_{H_2O} + \alpha_2 C_{C_3H_8O})} \quad (4)$$

$$r_{C_3H_8O} = - \left(\frac{k \exp - \frac{(Ea^*)}{RT} C_{C_3H_8O} C_{H_2O} \sqrt{e^{a,s}}}{\left(1 + A_{H_2O}^* \exp - \frac{Ea_{H_2O}^*}{RT} C_{H_2O}\right)^2} + \frac{k'' \exp - \frac{(Ea)}{RT} C_{C_3H_8O}}{\left(1 + A_{H_2O} \exp - \frac{Ea_{H_2O}}{RT} C_{H_2O}\right)} \right) \quad (5)$$

In Equation (4), $\alpha_1 = \frac{k_4 K_{A_{C_3H_8O}} [Sites] k_1 K_{H_2O} [S]}{\gamma} \sqrt{\frac{\phi}{k_3}}$ and $\alpha_2 = \frac{k_4 K_{A_{C_3H_8O}} [S]}{\gamma}$. In Equation (5), $k = \frac{k_{4.1} [S]^2 k_1 A_{C_3H_8O}^* A_{H_2O}^*}{\gamma} \sqrt{\frac{\phi}{k_3}}$ and $k'' = k_{4.2} [S] [S_1] A_{C_3H_8O} A_{O_2}$. A is the pre-exponential factor, Ea is the activation energy, and T and R are temperature and universal gas constant, respectively. k are kinetic constants (units depend on the reaction step) of specific stages of each reaction, while K are adsorption constants ($m^3 \text{ mol}^{-1}$). ϕ is the primary quantum yield ($\text{mol of photons}^{-1}$). In both equations, the kinetic study considered three levels for each factor. Under pure photocatalytic conditions, the concentration of C_3H_8O and water (defined as relative humidity) and the radiation intensity affecting the parameter $e^{a,s}$ in the equations were evaluated. Additionally, in Equation (5), the reaction temperature was also evaluated over a range of 220 °C to 270 °C.

Figure 5A–C presents the results of the thermo-photodegradation of 2-propanol using the reactor schematically shown in Figure 5D. The reactor is an annular reactor, where the gas flows through the annular space. The radiation sources were four UV fluorescent lamps (365 nm), and the temperature was increased using a cartridge heater. In this study, the ceria-titania system has an enhancement factor of approximately 1.32 and 1.33 with respect to the parent systems (TiO_2 and Ce_xO_x) in the kinetic constants controlling the active

species (oxygen and hydroxyl-type radical species, respectively) responsible for attacking the 2-propanol molecule in the degradation process. In addition, the local superficial rate of photon absorption was evaluated (Figure 5E). The left panel corresponds to the TiO₂ sample, while the right panel corresponds to the composite system that optimizes the catalytic response (CeO₂/TiO₂ composite material).

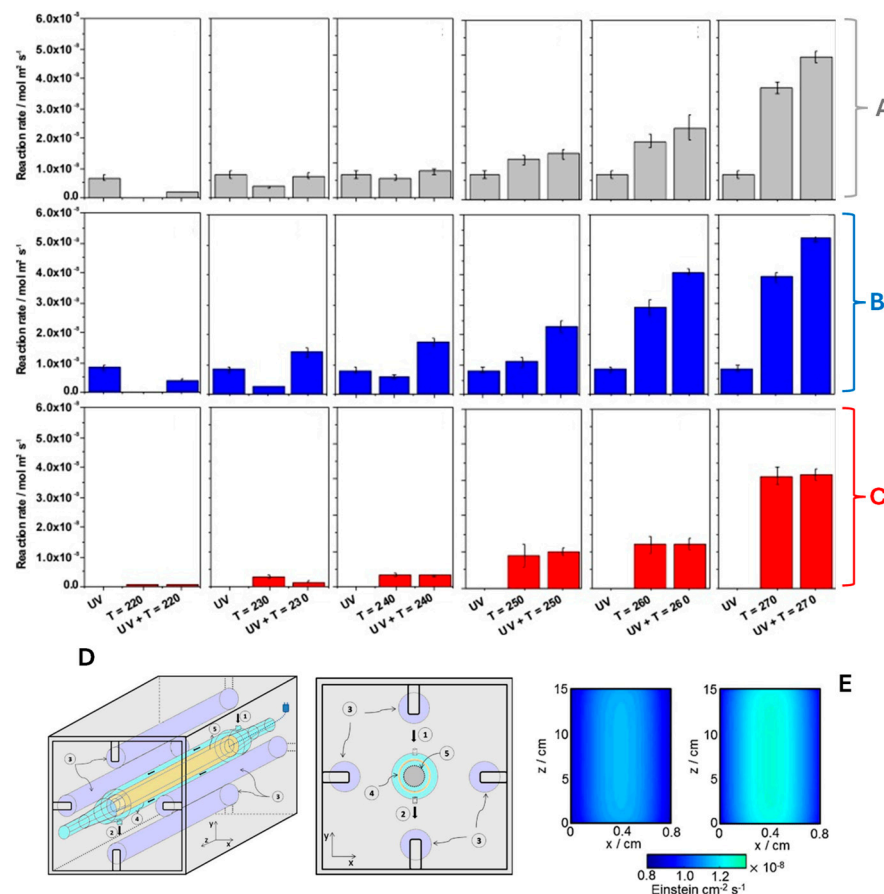


Figure 5. Catalytic activity of the TiO₂ (A), CeO_x/TiO₂ (B), and CeO_x samples (C) under combined light (UV) and temperature conditions (up to 270 °C). (D) Thermo-photocatalytic reactor (1: gas inlet, 2: gas outlet, 3: UV lamp, 4: catalyst sample, 5: cartridge heater). (E) Surface photon absorption rate under UV illumination (365 nm): left panel TiO₂, right panel ceria-titania sample. Adapted from [36].

In addition to quantum efficiency, there are other definitions commonly used to evaluate the behavior of photocatalytic reaction systems. The radiation incidence efficiency (η_I) depends directly on both the reactor configuration and the system's optical properties and can be defined by Equation (6) [77–79]. On the other hand, the radiation absorption efficiency (η_A) is a relation between the absorption (LSRPA or LVRPA) with the incident radiation flow at the catalytic film (Equation (7)) [77–79]. This parameter displays a strong spectral dependence and allows quantitative comparisons concerning different light sources and samples. While quantum efficiency is commonly used to evaluate or compare the performance of catalysts, these last two definitions are particularly interesting for assessing the design efficiency in terms of how effectively the design delivers radiation to the sample or how much of the incident radiation is effectively absorbed by the material. In Equations (6) and (7), q is the net radiation flux and P is the emission power.

$$\eta_I = \frac{\int_A \int_\lambda q_\lambda d\lambda dA}{\int_\lambda P_{\lambda,L} d\lambda} \times 100 \quad (6)$$

$$\eta_A = \frac{\int_A \int_{\lambda} LSRPA \, d\lambda \, dA}{\int_A \int_{\lambda} q_{\lambda} \, d\lambda \, dA} \times 100 \quad (7)$$

A similar analysis allows for the definition of heat transfer efficiency in thermo-photocatalytic schemes. Heat transfer efficiency would measure the proportion of total heat generated within the reactor that is effectively transferred to the catalyst/reaction. This efficiency is influenced by factors such as the thermal conductivity of materials, heat losses due to convection and radiation, and the overall design of the reactor to facilitate efficient heat transfer. Therefore, in reactor design, both radiation incidence efficiency and heat transfer efficiency are pivotal for optimizing system performance in which light and temperature are used.

Radiation incidence efficiency ensures that the energy emitted by the lamps is effectively utilized in the catalytic process, while heat transfer efficiency maximizes the useful heat transferred to the catalytic system. A comprehensive evaluation for the development of a thermo-photocatalytic system (catalytic materials and reactors) must obviously consider the efficiency of both radiation sources. Additionally, a balance between the consumption associated with radiation sources and the operation at high temperatures must be considered. For this, the identification of additive or synergistic effects will need to be carefully evaluated. Furthermore, the possibility of using solar light (zero costs in luminous radiation) or photo (auto-thermal) systems (zero costs in heating the reactor) are presented as extreme cases in relation to the use of energy sources. Solar light can provide a sustainable and cost-effective source of radiation, eliminating the need for artificial lighting. Self-thermal systems can leverage the heat generated within the reactor itself, reducing the need for external heating sources and potentially increasing overall system efficiency [30].

An analysis of the literature focused on the design of photocatalytic reactors and thermal reactors allows for the identification of the main variables generally discussed regarding efficiency in terms of the use of radiation or thermal energy (using resistances). The main ideas are summarized in Table 2. However, it should be noted that there are very few contributions focused on the energy optimization of thermo-photocatalytic reactors.

Table 2. Main aspects affecting the efficient use of heat and light in thermo-photo reactors.

Efficient Use of Temperature (Using Thermal Resistances)	Efficient Use of Light Irradiation (Using Artificial Lighting Sources)
Uniform Heat Distribution: Ensure resistances are evenly distributed around the reactor to avoid hot and cold spots, maintaining a consistent temperature throughout the reactor surface/volume. An annular reactor with a high-load cartridge-type resistance in the center could provide a valid alternative.	Uniform Light Distribution: Ensure lamps are arranged to distribute light evenly throughout the reactor. This may involve using reflectors or diffusers to maximize the catalyst's exposure to light. Tubular reactors with fluorescent lamps or flat reactors with correctly positioned lamps provide homogeneously illuminated surfaces.
Precise Temperature Control: Use high-precision temperature sensors and a PID (Proportional-Integral-Derivative) control system to adjust the power of the resistances in real-time, maintaining the desired temperature with minimal fluctuation.	Type of Lamps: Use efficient lamps that emit in the appropriate wavelength range for the photocatalytic reaction. The proper characterization of the optical properties (band gap, light penetration, LSRPA/LVRPA) of the semiconductors used can help to correctly define irradiation conditions.
Thermal Insulation: Implement sufficient thermal insulation around the reactor to minimize heat loss, improving energy efficiency and reducing the power consumption of the resistances.	Temperature Control: Maintain an appropriate temperature of the light source. This may require additional cooling or heating systems for the lamps. This is one of the main bottlenecks for the design of thermo-photo reactors. Most light sources work efficiently or are not damaged below 50 °C.

Table 2. Cont.

Efficient Use of Temperature (Using Thermal Resistances)	Efficient Use of Light Irradiation (Using Artificial Lighting Sources)
Catalyst Positioning: Position the catalyst to ensure it is in an optimal location for effective temperature control. This can be achieved by using supports that hold the catalyst in the best position within the reactor to avoid overheating or underheating.	Catalyst Positioning: Position the catalyst to maximize its exposure to light. This can be achieved by using supports that hold the catalyst in an optimal position within the reactor in relation to the illumination. In systems with supported catalysts, the thickness of the catalyst layer can be controlled. As discussed before, it is especially important that the solid is efficiently exposed to radiation. In reactors in which the catalyst is distributed in the volume (e.g., catalytic suspension, a suitable mixing should be quarantine).

4. The Case of a Flat Thermo-Photo Reactor

In this section, a flat thermo-photocatalytic reaction system is analyzed. The plate thermo-photo reactor design offers distinct advantages regarding the efficiency of light and temperature distribution. Its planar configuration promotes uniform light irradiation across the catalyst surface, a feature that is essential for maximizing photocatalytic efficiency by minimizing “dead zones” or regions with suboptimal light exposure. This homogeneity permits a reduction in catalyst material requirements, thereby conserving energy and materials. Such uniformity is particularly beneficial for reactions requiring high selectivity. Furthermore, the plate reactor’s design facilitates precise temperature control, an essential factor for thermo-photocatalytic processes where the interplay of temperature and light is crucial. Due to the proximity of heating elements (heating in contact with the plate in which the sample is deposited) to the catalyst, the reactor achieves rapid and consistent temperature adjustments, preventing the formation of thermal gradients that could otherwise reduce reaction efficiency or generate undesirable byproducts. Maintaining both temperature and light at optimal levels across the catalytic surface enhances catalytic activity, selectivity, and quantum efficiency. Additionally, the homogeneity in light and temperature profiles simplifies intrinsic kinetic analysis, as averaged kinetic data more accurately represent the reaction process under these consistent conditions, reducing the need for complex corrections and supporting robust modeling of reaction mechanisms and catalytic performance.

However, despite these advantages, the planar geometry inherently restricts the reactor’s capacity to process large reactant volumes, limiting its scalability for industrial applications. In large-scale systems that require substantial reactant volumes, the planar configuration may reduce volumetric efficiency, thereby diminishing productivity in terms of product yield per unit of time. Consequently, the plate reactor may be non-optimal for large-scale operations.

As a first approximation for intrinsic kinetics studies and calculation of quantum efficiency-like parameters, Figure 6 shows temperature (A) and photon rate (B) profiles for a plate thermo-photo reactor in which the catalysis is deposited on a 20 cm × 20 cm quartz surface. Both models have been developed using Matlab2013a. These profiles correspond to a catalyst film deposited on a plate in a reactor system like that described in Figure 3E, with the difference being that instead of fluorescent lamps, the irradiation comes from a 5 × 5 LED configuration and, additionally, the plate (where the catalyst is deposited) is heated by a 5 × 5 cm resistance.

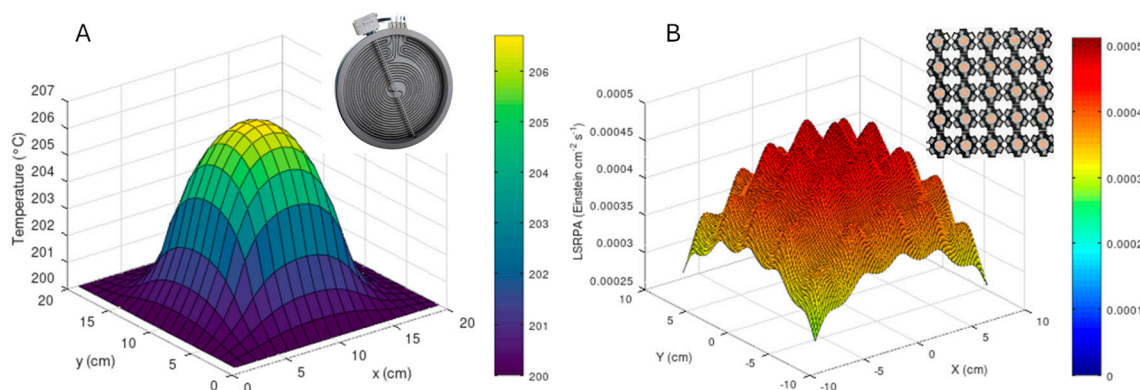


Figure 6. Temperature profile (A) and local superficial rate of photon absorption (B) obtained for a 20 cm × 20 cm catalytic film of a flat thermo-photo reactor.

For temperature profile (Figure 6A), the model is based on a simplified two-dimensional heat diffusion equation, solved using an explicit finite-difference method. The equation describes the temporal and spatial evolution of temperature (T) in the plate: $\frac{dT}{dt} = \alpha \left(\frac{d^2T}{dx^2} + \frac{d^2T}{dy^2} \right)$, where $\alpha = \frac{k}{\rho C_p}$ is the thermal diffusivity, derived from the thermal conductivity (k), density (ρ), and specific heat capacity (C_p) of the material. The plate, assumed to be homogeneous and isotropic, has an initial uniform temperature and is heated by a localized heat source covering a 5×5 cm area at its center. The model assumes perfect thermal contact between the heat source and the plate, neglects convective and radiative heat losses, and applies zero-flux (insulated) boundary conditions to simulate an idealized scenario. The temperature distribution is computed iteratively over time until the steady-state or desired simulation time is reached. To obtain the LSRPA profile (Figure 6B), the model calculates the spatial distribution of radiation in a photocatalytic reactor illuminated by an LED array, analyzing the intensity at the reactor surface and across varying depths. It assumes LEDs emit a Gaussian spectral distribution centered at 365 nm, with a full width at half maximum (FWHM) of 30 nm, and uniformly radiate within a specified viewing angle (70 degree). The medium's absorption is characterized using a wavelength-dependent absorption coefficient, while scattering effects and medium heterogeneities are neglected. LED positions are evenly spaced over a flat reactor surface. Thermal effects and changes in optical properties with temperature or light exposure are also excluded. As aforementioned, with profiles exhibiting moderate variations (e.g., $T \approx 205$ °C and $\text{LSRPA} \approx 3 \times 10^{-5}$ Einstein $\text{cm}^{-2} \text{s}^{-1}$), TOF, quantum efficiency and intrinsic kinetic studies, with proper settings for combined processes with light and temperature, could be considered to evaluate the thermo-photocatalytic process.

5. Conclusions and Future Perspectives

The field of thermo-photocatalytic processes is continuously evolving, with several promising directions for future development. Current research focuses on the design and synthesis of new catalytic materials with enhanced optical and thermal properties. Although this perspective article does not delve into the preparation methods and properties of new efficient materials under mixed light–temperature conditions, several trends in this field can be identified. The use of nanomaterials, such as carbon nanotubes and quantum dots, and hybrid structures, such as metal oxide heterostructures and organometallic compounds, could offer innovative solutions to overcome current limitations. Other materials, such as appropriately functionalized perovskites and carbon-based structures, show significant potential in thermo-photocatalysis due to their exceptional optical absorption, charge carrier mobility, and thermal stability.

The optimization and development of energy-efficient reactors are much less studied. If, as appears to be the case, schemes with combined light and temperature sources significantly improve those using a single source (light or temperature), there will be an increasing emphasis on optimizing the energy efficiency of these processes. The implementation of advanced computational models will allow for a better understanding and prediction of catalyst behavior under various conditions, facilitating the design of more efficient and customized processes. In this way, it is expected that future innovation in reactor design will allow for better management of heat and light, improving the efficiency and scalability of the processes.

More attention should be paid to how systems are analyzed under light and temperature. The determination of optical properties of catalysts at the working temperature and the efficient and homogeneous use of temperature and light profiles should be carefully addressed. Further progress should also be made in unifying the criteria for evaluating catalytic properties, taking into account the definitions of turnover frequency and quantum efficiency.

In systems with supported catalysts, like those analyzed in this work, special attention must be paid to providing a homogeneous radiation and temperature profile of the samples. Working under controlled conditions, in terms of light absorption and heat absorbed by the catalyst, will largely determine the proper functioning of the materials and the phenomena that define the synergistic effect (e.g., charge mobility, redox potential, active sites, kinetic driving force, etc.). Flat reaction systems, where the radiation reaches the catalyst surface and thus the photon absorption rate can be easily controlled, as well as the possibility of easily heating the catalyst support, make this configuration beneficial in laboratory reactors. Other schemes, such as annular systems with an internal heating source, are, on the other hand, more efficient in terms of heat transfer efficiency.

The integration of solar radiation into traditional thermal schemes also seems to be one of the most efficient routes in schemes under thermal and light radiation. Furthermore, by using efficient radiation sources such as LEDs, energy consumption associated with light can be considerably reduced. If well-designed facilities are developed in the coming years, which address the main bottlenecks for the development of the combined use of light and temperature, one could expect an expansion of the industrial and environmental applications of these processes, including the degradation of pollutants, the production of hydrogen and other clean fuels, and the synthesis of high value-added chemicals.

Funding: This research was funded by the 2024 Leonardo Grant for Scientific Research and Cultural Creation from the BBVA Foundation.

Data Availability Statement: Data presented in this study are available on request.

Conflicts of Interest: The author declares no conflicts of interest.

References

1. Oro, L.A. Pushing the Boundaries of Catalysis. *ChemCatChem* **2009**, *1*, 6. [[CrossRef](#)]
2. Rodríguez-Padrón, D.; Puente-Santiago, A.R.; Balu, A.M.; Muñoz-Batista, M.J.; Luque, R. Environmental Catalysis: Present and Future. *ChemCatChem* **2019**, *11*, 18–38. [[CrossRef](#)]
3. Bao, X. Preface: Catalysis—Key to a Sustainable Future. *Natl. Sci. Rev.* **2015**, *2*, 137. [[CrossRef](#)]
4. Sheldon, R.A. Engineering a More Sustainable World through Catalysis and Green Chemistry. *J. R. Soc. Interface* **2016**, *13*. [[CrossRef](#)] [[PubMed](#)]
5. Gibson, P. Catalysis for Fuels: Concluding Remarks. *Faraday Discuss.* **2017**, *197*, 547–555. [[CrossRef](#)]
6. Gong, J.; Luque, R. Catalysis for Production of Renewable Energy. *Chem. Soc. Rev.* **2014**, *43*, 7466–7468. [[CrossRef](#)]
7. Gates, B.C.; Huber, G.W.; Marshall, C.L.; Ross, P.N.; Siirola, J.; Wang, Y. Catalysts for Emerging Energy Applications. *MRS Bull.* **2008**, *33*, 429–435. [[CrossRef](#)]

8. Li, C.; Zhao, X.; Wang, A.; Huber, G.W.; Zhang, T. Catalytic Transformation of Lignin for the Production of Chemicals and Fuels. *Chem. Rev.* **2015**, *115*, 11559–11624. [\[CrossRef\]](#)
9. Climent, M.J.; Corma, A.; Iborra, S. Heterogeneous Catalysts for the One-Pot Synthesis of Chemicals and Fine Chemicals. *Chem. Rev.* **2011**, *111*, 1072–1133. [\[CrossRef\]](#) [\[PubMed\]](#)
10. Li, P.; Terrett, J.A.; Zbieg, J.R. Visible-Light Photocatalysis as an Enabling Technology for Drug Discovery: A Paradigm Shift for Chemical Reactivity. *ACS Med. Chem. Lett.* **2020**, *11*, 2120–2130. [\[CrossRef\]](#)
11. Hayler, J.D.; Leahy, D.K.; Simmons, E.M. A Pharmaceutical Industry Perspective on Sustainable Metal Catalysis. *Organometallics* **2018**, *38*, 36–46. [\[CrossRef\]](#)
12. Sheldon, R.A. E Factors, Green Chemistry and Catalysis: An Odyssey. *Chem. Commun.* **2008**, 3352–3365. [\[CrossRef\]](#) [\[PubMed\]](#)
13. Sheldon, R.A. Fundamentals of Green Chemistry: Efficiency in Reaction Design. *Chem. Soc. Rev.* **2012**, *41*, 1437–1451. [\[CrossRef\]](#)
14. Leem, Y.C.; Myoung, N.S.; Hong, S.H.; Jeong, S.; Seo, O.; Park, S.J.; Yim, S.Y.; Kim, J.H. Near-UV Light Emitting Diode with on-Chip Photocatalysts for Purification Applications. *Nanoscale Adv.* **2022**, *4*, 3585–3591. [\[CrossRef\]](#) [\[PubMed\]](#)
15. Rouhani, S.; Taghipour, F. Photocatalytic Oxidation of Volatile Organic Compounds (VOCs) in Air Using Ultraviolet Light-Emitting Diodes (UV-LEDs). *Chem. Eng. Sci.* **2023**, *272*, 118617. [\[CrossRef\]](#)
16. Ferreira, L.C.; Fernandes, J.R.; Rodríguez-Chueca, J.; Peres, J.A.; Lucas, M.S.; Tavares, P.B. Photocatalytic Degradation of an Agro-Industrial Wastewater Model Compound Using a UV LEDs System: Kinetic Study. *J. Environ. Manag.* **2020**, *269*, 110740. [\[CrossRef\]](#)
17. Chen, C.H.; Peng, Y.P. LED-Driven Photocatalysis of Toluene, Trichloroethylene and Formaldehyde by Cuprous Oxide Modified Titanate Nanotube Arrays. *Chemosphere* **2022**, *286*, 131608. [\[CrossRef\]](#)
18. Lang, X.; Chen, X.; Zhao, J. Heterogeneous Visible Light Photocatalysis for Selective Organic Transformations. *Chem. Soc. Rev.* **2013**, *43*, 473–486. [\[CrossRef\]](#) [\[PubMed\]](#)
19. Yang, X.; Wang, D. Photocatalysis: From Fundamental Principles to Materials and Applications. *ACS Appl. Energy Mater.* **2018**, *1*, 6657–6693. [\[CrossRef\]](#)
20. Mohamadpour, F.; Amani, A.M. Photocatalytic Systems: Reactions, Mechanism, and Applications. *RSC Adv.* **2024**, *14*, 20609–20645. [\[CrossRef\]](#)
21. Li, X.; Chen, Y.; Tao, Y.; Shen, L.; Xu, Z.; Bian, Z.; Li, H. Challenges of Photocatalysis and Their Coping Strategies. *Chem. Catal.* **2022**, *2*, 1315–1345. [\[CrossRef\]](#)
22. Qu, Y.; Duan, X. Progress, Challenge and Perspective of Heterogeneous Photocatalysts. *Chem. Soc. Rev.* **2013**, *42*, 2568–2580. [\[CrossRef\]](#)
23. Kubacka, A.; Fernández-García, M.; Colón, G. Advanced Nanoarchitectures for Solar Photocatalytic Applications. *Chem. Rev.* **2012**, *112*, 1555–1614. [\[CrossRef\]](#) [\[PubMed\]](#)
24. Song, X.; Shan, X.; Xue, H.; Li, X.; Liu, R.; Kong, J.; Zuo, Z.; Su, X.; Zhang, Q.; Yin, Y.; et al. Advances in Photothermal Catalysis: Mechanisms, Materials, and Environmental Applications. *ACS Appl. Nano Mater.* **2024**, *7*, 26489–26514. [\[CrossRef\]](#)
25. Nair, V.; Muñoz-Batista, M.J.; Fernández-García, M.; Luque, R.; Colmenares, J.C. Thermo-Photocatalysis: Environmental and Energy Applications. *ChemSusChem* **2019**, *12*, 2098–2116. [\[CrossRef\]](#)
26. Fang, S.; Hu, Y.H. Thermo-Photo Catalysis: A Whole Greater than the Sum of Its Parts. *Chem. Soc. Rev.* **2022**, *51*, 3609–3647. [\[CrossRef\]](#)
27. Mateo, D.; Cerrillo, J.L.; Durini, S.; Gascon, J. Fundamentals and Applications of Photo-Thermal Catalysis. *Chem. Soc. Rev.* **2021**, *50*, 2173–2210. [\[CrossRef\]](#)
28. Yu, X.; Zhao, C.; Chen, Z.; Yang, L.; Zhu, B.; Fan, S.; Zhang, J.; Chen, C. Advances in Photothermal Catalysis for Air Pollutants. *Chem. Eng. J.* **2024**, *486*, 150192. [\[CrossRef\]](#)
29. Xiao, Z.; Li, P.; Zhang, H.; Zhang, S.; Tan, X.; Ye, F.; Gu, J.; Zou, J.; Wang, D. A Comprehensive Review on Photo-Thermal Co-Catalytic Reduction of CO₂ to Value-Added Chemicals. *Fuel* **2024**, *362*, 130906. [\[CrossRef\]](#)
30. Keller, N.; Ivanez, J.; Highfield, J.; Ruppert, A.M. Photo-/Thermal Synergies in Heterogeneous Catalysis: Towards Low-Temperature (Solar-Driven) Processing for Sustainable Energy and Chemicals. *Appl. Catal. B* **2021**, *296*, 120320. [\[CrossRef\]](#)
31. Lv, H.; Macharia, D.K.; Liu, Z.; Zhang, L.; Yu, C.; Lu, C.; Liu, H.; Zhang, Y.; Chen, Z. Au-Loaded ZIF-8 Derived Porous Carbon with Improved Photothermal Catalysis Ability from Interfacial Heating Instead of Hot-Electrons. *Chem. Eng. J.* **2024**, *482*, 148963. [\[CrossRef\]](#)
32. Žerjav, G.; Say, Z.; Zavašnik, J.; Finšgar, M.; Langhammer, C.; Pintar, A. Photo, Thermal and Photothermal Activity of TiO₂ Supported Pt Catalysts for Plasmon-Driven Environmental Applications. *J. Environ. Chem. Eng.* **2023**, *11*, 110209. [\[CrossRef\]](#)
33. Caudillo-Flores, U.; Sayago, R.; Ares-Dorado, A.; Fuentes-Moyado, S.; Fernández-García, M.; Kubacka, A. Green Thermo-Photo Catalytic Production of Syngas Using Pd/Nb-TiO₂ Catalysts. *ACS Sustain. Chem. Eng.* **2023**, *11*, 3896–3906. [\[CrossRef\]](#) [\[PubMed\]](#)
34. Paulista, L.O.; Ferreira, A.F.P.; Castanheira, B.; Đolić, M.B.; Martins, R.J.E.; Boaventura, R.A.R.; Vilar, V.J.P.; Silva, T.F.C.V. Solar-Driven Thermo-Photocatalytic CO₂ Methanation over a Structured RuO₂:TiO₂/SBA-15 Nanocomposite at Low Temperature. *Appl. Catal. B* **2024**, *340*, 123232. [\[CrossRef\]](#)

35. Zheng, J.; Lu, L.; Lebedev, K.; Wu, S.; Zhao, P.; McPherson, I.J.; Wu, T.S.; Kato, R.; Li, Y.; Ho, P.L.; et al. Fe on Molecular-Layer MoS₂ as Inorganic Fe-S₂-Mo Motifs for Light-Driven Nitrogen Fixation to Ammonia at Elevated Temperatures. *Chem. Catal.* **2021**, *1*, 162–182. [\[CrossRef\]](#)
36. Muñoz-Batista, M.J.; Eslava-Castillo, A.M.; Kubacka, A.; Fernández-García, M. Thermo-Photo Degradation of 2-Propanol Using a Composite Ceria-Titania Catalyst: Physico-Chemical Interpretation from a Kinetic Model. *Appl. Catal. B* **2018**, *225*, 298–306. [\[CrossRef\]](#)
37. Kozuch, S.; Martin, J.M.L. “Turning over” Definitions in Catalytic Cycles. *ACS Catal.* **2012**, *2*, 2787–2794. [\[CrossRef\]](#)
38. Caudillo-Flores, U.; Muñoz-Batista, M.J.; Fernández-García, M.; Kubacka, A. Recent Progress in the Quantitative Assessment and Interpretation of Photoactivity. *Catal. Rev.* **2024**, *66*, 531–585. [\[CrossRef\]](#)
39. Braslavsky, S.E.; Braun, A.M.; Cassano, A.E.; Emeline, A.V.; Litter, M.I.; Palmisano, L.; Parmon, V.N.; Serpone, N. Glossary of Terms Used in Photocatalysis and Radiation Catalysis (IUPAC Recommendations 2011). *Pure Appl. Chem.* **2011**, *83*, 931–1014. [\[CrossRef\]](#)
40. Serpone, N.; Terzian, R.; Lawless, D.; Kennepohl, P.; Sauvé, G. On the Usage of Turnover Numbers and Quantum Yields in Heterogeneous Photocatalysis. *J. Photochem. Photobiol. A Chem.* **1993**, *73*, 11–16. [\[CrossRef\]](#)
41. Serpone, N. Relative Photonic Efficiencies and Quantum Yields in Heterogeneous Photocatalysis. *J. Adv. Oxid. Technol.* **1997**, *2*, 203–216. [\[CrossRef\]](#)
42. Serpone, N.; Salinaro, A. Terminology, Relative Photonic Efficiencies and Quantum Yields in Heterogeneous Photocatalysis. Part I: Suggested Protocol (Technical Report). *Pure Appl. Chem.* **1999**, *71*, 303–320. [\[CrossRef\]](#)
43. Muñoz-Batista, M.J.; Kubacka, A.; Hungria, A.B.; Fernández-García, M. Heterogeneous Photocatalysis: Light-Matter Interaction and Chemical Effects in Quantum Efficiency Calculations. *J. Catal.* **2015**, *330*, 154–166. [\[CrossRef\]](#)
44. Scott, T.; Zhao, H.; Deng, W.; Feng, X.; Li, Y. Photocatalytic Degradation of Phenol in Water under Simulated Sunlight by an Ultrathin MgO Coated Ag/TiO₂ Nanocomposite. *Chemosphere* **2019**, *216*, 1–8. [\[CrossRef\]](#)
45. Wei, X.; Xiang, H.; Xu, Y.; Wang, Z.; Chen, J. Photocatalytic Modeling for Maximizing Utilization of Real-Time Changing Sunlight and Rationalizing Evaluation. *AIChE J.* **2023**, *69*, e17985. [\[CrossRef\]](#)
46. Prier, C.K.; Rankic, D.A.; MacMillan, D.W.C. Visible Light Photoredox Catalysis with Transition Metal Complexes: Applications in Organic Synthesis. *Chem. Rev.* **2013**, *113*, 5322–5363. [\[CrossRef\]](#) [\[PubMed\]](#)
47. Baia, M.; Gajda-Schrantz, K.; Shen, S.; Stathatos, E. Progress and Perspectives in Visible-Light-Driven Photocatalysis. *Int. J. Photoenergy* **2013**, *2013*, 314187. [\[CrossRef\]](#)
48. Binjhade, R.; Mondal, R.; Mondal, S. Continuous Photocatalytic Reactor: Critical Review on the Design and Performance. *J. Environ. Chem. Eng.* **2022**, *10*, 107746. [\[CrossRef\]](#)
49. Birnie, M.; Riffat, S.; Gillott, M. Photocatalytic Reactors: Design for Effective Air Purification. *Int. J. Low-Carbon Technol.* **2006**, *1*, 47–58. [\[CrossRef\]](#)
50. Mendret, J.; Brosillon, S. Advances in Photocatalytic Membrane Reactor. *Membranes* **2023**, *13*, 541. [\[CrossRef\]](#) [\[PubMed\]](#)
51. Ibadon, A.O.; Fitzpatrick, P. Heterogeneous Photocatalysis: Recent Advances and Applications. *Catalysts* **2013**, *3*, 189–218. [\[CrossRef\]](#)
52. Singh, J.A.; Cao, A.; Schumann, J.; Wang, T.; Nørskov, J.K.; Abild-Pedersen, F.; Bent, S.F. Theoretical and Experimental Studies of CoGa Catalysts for the Hydrogenation of CO₂ to Methanol. *Catal. Lett.* **2018**, *148*, 3583–3591. [\[CrossRef\]](#)
53. Cho, Y.; Yamaguchi, A.; Uehara, R.; Yasuhara, S.; Hoshina, T.; Miyauchi, M. Temperature Dependence on Bandgap of Semiconductor Photocatalysts. *J. Chem. Phys.* **2020**, *152*, 231101. [\[CrossRef\]](#) [\[PubMed\]](#)
54. Kozuch, S.; Shaik, S. How to Conceptualize Catalytic Cycles? The Energetic Span Model. *Acc. Chem. Res.* **2011**, *44*, 101–110. [\[CrossRef\]](#)
55. Kozuch, S. A Refinement of Everyday Thinking: The Energetic Span Model for Kinetic Assessment of Catalytic Cycles. *Wiley Interdiscip. Rev. Comput. Mol. Sci.* **2012**, *2*, 795–815. [\[CrossRef\]](#)
56. Wodrich, M.D.; Sawatlon, B.; Solel, E.; Kozuch, S.; Corminboeuf, C. Activity-Based Screening of Homogeneous Catalysts through the Rapid Assessment of Theoretically Derived Turnover Frequencies. *ACS Catal.* **2019**, *9*, 5716–5725. [\[CrossRef\]](#)
57. Manassero, A.; Alfano, O.M.; Satuf, M.L. Radiation Modeling and Performance Evaluation of a UV-LED Photocatalytic Reactor for Water Treatment. *J. Photochem. Photobiol. A Chem.* **2023**, *436*, 114367. [\[CrossRef\]](#)
58. Salvadores, F.; Brandi, R.J.; Alfano, O.M.; de los Milagros Ballari, M. Modelling and Experimental Validation of Reaction Chamber Simulating Indoor Air Decontamination by Photocatalytic Paint. *Appl. Catal. A Gen.* **2023**, *663*, 119285. [\[CrossRef\]](#)
59. Mueses, M.A.; Colina-Márquez, J.; Machuca-Martínez, F.; Li Puma, G. Recent Advances on Modeling of Solar Heterogeneous Photocatalytic Reactors Applied for Degradation of Pharmaceuticals and Emerging Organic Contaminants in Water. *Curr. Opin. Green Sustain. Chem.* **2021**, *30*, 100486. [\[CrossRef\]](#)
60. Lara-Ramos, J.A.; Sánchez-Gómez, K.; Valencia-Rincón, D.; Diaz-Angulo, J.; Mueses, M.; Machuca-Martínez, F. Intensification of the O₃/TiO₂/UV Advanced Oxidation Process Using a Modified Flotation Cell. *Photochem. Photobiol. Sci.* **2019**, *18*, 920–928. [\[CrossRef\]](#) [\[PubMed\]](#)

61. Wang, D.; Mueses, M.A.; Márquez, J.A.C.; Machuca-Martínez, F.; Grčić, I.; Peralta Muniz Moreira, R.; Li Puma, G. Engineering and Modeling Perspectives on Photocatalytic Reactors for Water Treatment. *Water Res.* **2021**, *202*, 117421. [[CrossRef](#)] [[PubMed](#)]
62. Moreno-SanSegundo, J.; Casado, C.; Marugán, J. Enhanced Numerical Simulation of Photocatalytic Reactors with an Improved Solver for the Radiative Transfer Equation. *Chem. Eng. J.* **2020**, *388*, 124183. [[CrossRef](#)]
63. Ramyashree, M.S.; Nandy, A.; Bohari, Y.R.; Pramodh, M.; Kumar, S.H.; Shanmuga Priya, S.; Sudhakar, K. Modeling and Simulation of Reactors for Methanol Production by CO₂ Reduction: A Comparative Study. *Results Eng.* **2024**, *23*, 102306. [[CrossRef](#)]
64. Quintana, M.A.; Solís, R.R.; Blázquez, G.; Calero, M.; Muñoz-Batista, M.J. Sulfonic Grafted Graphitic-like Carbon Nitride for the Improved Photocatalytic Production of Benzaldehyde in Water. *Appl. Surf. Sci.* **2024**, *656*, 159717. [[CrossRef](#)]
65. Quintana, M.A.; Picón, A.; Martín-Lara, M.Á.; Calero, M.; Muñoz-Batista, M.J.; Solís, R.R. Towards the Photocatalytic Production of Cinnamaldehyde with Phosphorous-Tailored Graphitic-like Carbon Nitride. *Appl. Catal. A Gen.* **2024**, *674*, 119607. [[CrossRef](#)]
66. Jimenez-Calvo, P.; Muñoz-Batista, M.J.; Isaacs, M.; Ramnarain, V.; Ihiawakrim, D.; Li, X.; Ángel Muñoz-Márquez, M.; Teobaldi, G.; Kociak, M.; Paineau, E. A Compact Photoreactor for Automated H₂ Photoproduction: Revisiting the (Pd, Pt, Au)/TiO₂ (P25) Schottky Junctions. *Chem. Eng. J.* **2023**, *459*, 141514. [[CrossRef](#)]
67. Muñoz-Batista, M.J.; Motta Meira, D.; Colón, G.; Kubacka, A.; Fernández-García, M. Phase-Contact Engineering in Mono- and Bimetallic Cu-Ni Co-Catalysts for Hydrogen Photocatalytic Materials. *Angew. Chem. Int. Ed.* **2018**, *57*, 1199–1203. [[CrossRef](#)]
68. Platero, F.; Caballero, A.; Colón, G. Tuning the Co-Catalyst Loading for the Optimization of Thermo-Photocatalytic Hydrogen Production over Cu/TiO₂. *Appl. Catal. A Gen.* **2022**, *643*, 118804. [[CrossRef](#)]
69. Muñoz-Batista, M.J.; Ballari, M.M.; Kubacka, A.; Alfano, O.M.; Fernández-García, M. Braiding Kinetics and Spectroscopy in Photo-Catalysis: The Spectro-Kinetic Approach. *Chem. Soc. Rev.* **2019**, *48*, 637–682. [[CrossRef](#)]
70. Xie, B.; Wong, R.J.; Tan, T.H.; Higham, M.; Gibson, E.K.; Decarolis, D.; Callison, J.; Aguey-Zinsou, K.F.; Bowker, M.; Catlow, C.R.A.; et al. Synergistic Ultraviolet and Visible Light Photo-Activation Enables Intensified Low-Temperature Methanol Synthesis over Copper/Zinc Oxide/Alumina. *Nat. Commun.* **2020**, *11*, 1615. [[CrossRef](#)] [[PubMed](#)]
71. Xie, B.; Kumar, P.; Tan, T.H.; Esmailpour, A.A.; Aguey-Zinsou, K.F.; Scott, J.; Amal, R. Doping-Mediated Metal-support Interaction Promotion toward Light-Assisted Methanol Production over Cu/ZnO/Al₂O₃. *ACS Catal.* **2021**, *11*, 5818–5828. [[CrossRef](#)]
72. Barba-Nieto, I.; Caudillo-Flores, U.; Gómez-Cerezo, M.N.; Kubacka, A.; Fernández-García, M. Boosting Pt/TiO₂ Hydrogen Photoproduction through Zr Doping of the Anatase Structure: A Spectroscopic and Mechanistic Study. *Chem. Eng. J.* **2020**, *398*, 125665. [[CrossRef](#)]
73. Obregón, S.; Muñoz-Batista, M.J.; Fernández-García, M.; Kubacka, A.; Colón, G. Cu–TiO₂ Systems for the Photocatalytic H₂ Production: Influence of Structural and Surface Support Features. *Appl. Catal. B* **2015**, *179*, 468–478. [[CrossRef](#)]
74. Alfano, O.M.; Cassano, A.E. Scaling-Up of Photoreactors: Applications to Advanced Oxidation Processes. *Adv. Chem. Eng.* **2009**, *36*, 229–287. [[CrossRef](#)]
75. Imoberdorf, G.E.; Irazoqui, H.A.; Alfano, O.M.; Cassano, A.E. Scaling-up from First Principles of a Photocatalytic Reactor for Air Pollution Remediation. *Chem. Eng. Sci.* **2007**, *62*, 793–804. [[CrossRef](#)]
76. Marugán, J.; van Grieken, R.; Cassano, A.E.; Alfano, O.M. Scaling-up of Slurry Reactors for the Photocatalytic Oxidation of Cyanide with TiO₂ and Silica-Supported TiO₂ Suspensions. *Catal. Today* **2009**, *144*, 87–93. [[CrossRef](#)]
77. Muñoz-Batista, M.J.; de los Milagros Ballari, M.; Kubacka, A.; Cassano, A.E.; Alfano, O.M.; Fernández-García, M. Acetaldehyde Degradation under UV and Visible Irradiation Using CeO₂–TiO₂ Composite Systems: Evaluation of the Photocatalytic Efficiencies. *Chem. Eng. J.* **2014**, *255*, 297–306. [[CrossRef](#)]
78. Imoberdorf, G.E.; Cassano, A.E.; Irazoqui, H.A.; Alfano, O.M. Optimal Design and Modeling of Annular Photocatalytic Wall Reactors. *Catal. Today* **2007**, *129*, 118–126. [[CrossRef](#)]
79. Passalía, C.; Alfano, O.M.; Brandi, R.J. Optimal Design of a Corrugated-Wall Photocatalytic Reactor Using Efficiencies in Series and Computational Fluid Dynamics (CFD) Modeling. *Ind. Eng. Chem. Res.* **2013**, *52*, 6916–6922. [[CrossRef](#)]

Disclaimer/Publisher's Note: The statements, opinions and data contained in all publications are solely those of the individual author(s) and contributor(s) and not of MDPI and/or the editor(s). MDPI and/or the editor(s) disclaim responsibility for any injury to people or property resulting from any ideas, methods, instructions or products referred to in the content.